Journal of Photochemistry, *19* (1982) 215 - 227

THE WAVELENGTH AND PRESSURE DEPENDENCE OF THE PHOTOLYSIS OF PROPIONALDEHYDE IN AIR

PAUL B. SHEPSON and JULIAN HEICKLEN

Department of Chemistry, Ionosphere Research Laboratory, and Center for Air Environment Studies, The Pennsylvania State University, University Park, PA 16802 (U.S.A.)

(Received November 13, 1981; in revised form January 13, 1982)

Summary

Propionaldehyde was photolyzed in air at 23 ± 1 °C at pressures up to 1 atm at several incident wavelengths: 334, 326, 313, 302, 280 and 254 nm. The two primary processes are

$$C_2H_5CHO + h\nu \rightarrow C_2H_5 + HCO \xrightarrow{O_2} HO_2 + CO \quad (1)$$

$$C_2H_5CHO + h\nu \rightarrow C_2H_6 + CO \quad (2)$$

The products measured were CO and C_2H_6, the former being a measure of the sum of both processes and the latter being a measure of molecular process (2). At all wavelengths $\Phi(CO) \approx 1.0$ in the low pressure limit.

Primary process (2) is significant only with incident radiation at 254 and 280 nm. Its low pressure quantum yield is 0.39 at both wavelengths. At 254 nm there is no pressure quenching of C_2H_6, but at 280 nm most, but not all, of the C_2H_6 can be pressure quenched with a half-quenching pressure of 47 Torr of air. We suggest that primary process (2) comes from upper vibrational levels of the ground and excited singlet states.

Primary process (1) is pressure quenched at all wavelengths. The pressure quenching follows Stern–Volmer quenching at 326, 302, 280 and 254 nm. However, at 334 and 313 nm, the Stern–Volmer quenching curves show a marked deviation from linearity, and two states with different decomposition rates are indicated. We interpret primary process (1) as coming from upper vibrational levels of the triplet state but with the less reactive vibrational states being more readily quenched than the more reactive vibrational states to the ground vibrational level of the triplet. The half-quenching pressures increase from about 24 Torr at 334 nm to 280 Torr at 254 nm for the fast quench and from 325 Torr at 334 nm to 610 Torr at 280 nm for the slow quench. The more reactive states appear only at 334, 313 and 280 nm and always give a low pressure quantum yield of 0.60.

At atmospheric pressure the average quantum yield for all six incident wavelengths for primary process (1) is 0.20 ± 0.08. This leads to atmospheric photodissociation coefficients of about 1.3×10^{-5} s and about 9.7×10^{-6} s^{-1} for solar zenith angles of 30° and 58.18° respectively.

0047-2670/82/0000-0000/$02.75

1. Introduction

It is well known that the photolysis of the low molecular weight aliphatic aldehydes is an important source of free-radical production in polluted urban atmospheres [1]. However, there is a general lack of data on the primary process quantum yields as a function of wavelength and pressure, particularly for aldehydes other than formaldehyde. This information is essential for the purposes of tropospheric modeling.

There are two primary processes of importance in the photolysis of aldehydes, a radical process and a molecular process [2]:

$$RCHO + h\nu \rightarrow R + HCO \quad (1)$$

$$RCHO + h\nu \rightarrow RH + CO \quad (2)$$

A considerable amount of work has been done in the area of formaldehyde photolysis [3]. The result generally agreed upon is that the quantum yield ϕ_1 for process (1) increases from 0.0 at 338 nm to a maximum of about 0.7 at 305 nm, and then begins to fall off again in going to shorter wavelengths. The sum of $\phi_1 + \phi_2$ appears to be unity in the wavelength range between 280 and 330 nm.

Gill and Atkinson [4] have studied the wavelength dependence for HCO radical production from acetaldehyde photolysis at 10 Torr total pressure. They have found that the relative HCO quantum yields increase sharply from a threshold at 320 nm to a maximum at about 310 nm (where ϕ_1 is presumably unity) and then slowly fall off in going to shorter wavelengths. The quantum yield for process (2) has been found to be unimportant at wavelengths above about 300 nm but increases as the wavelength decreases to a value of 0.64 at 254 nm [2]. The work of Gill and Atkinson also indicates that the excited state lifetimes have a marked wavelength dependence, and this, taken with the ϕ_1 dependence, demonstrates a complicated and dramatic wavelength dependence of the various primary processes.

Few quantitative studies of propionaldehyde photolysis have been done. Blacet and Pitts [5] have studied the photolysis of propionaldehyde in the wavelength region 238 - 334 nm. In general they found that process (1) decreased and process (2) increased in importance as the wavelength was decreased. The sum of their measured primary process quantum yields did not equal unity, however, presumably because of excited state quenching by added I_2. Hansen and Lee [6] have found that the fluorescence quantum yield is unimportant over most of this wavelength range. Recent work done in our laboratory [7] at 313 nm indicates that ϕ_1 is unity at low pressures but that the excited state precursor to radical formation is pressure quenched, an effect also found in acetaldehyde photolysis by Weaver *et al.* [8].

It is the purpose of this work to determine the quantum yields for processes (1) and (2) as a function of pressure in air over the wavelength range 254 - 334 nm. Since all experiments were done in the presence of air, the formyl radicals produced in process (1) react to produce CO [9, 10]:

$$HCO + O_2 \rightarrow CO + HO_2 \quad (3)$$

Therefore measurements of the CO quantum yields provide a direct measure of the total quantum yields for processes (1) and (2). Primary process (2) is the only source of C_2H_6 in our system, and therefore the C_2H_6 quantum yield is a direct measure of this process.

2. Experimental details

The photolysis of propionaldehyde vapor was performed in a 1100 cm^3 cylindrical Pyrex cell fitted with quartz windows 9 cm in diameter. All experiments were carried out with 10.1 ± 0.1 Torr of propionaldehyde and at a temperature of 23 ± 1 °C. Gases were admitted to the reaction cell through a conventional grease-free vacuum line. The total pressure in the cell was brought to the desired value by adding various amounts of dry air.

The CO and C_2H_6 produced were determined by expansion to a gas chromatograph sample loop after irradiation. CO was then separated on stainless steel columns 5 ft long with an outside diameter of 0.25 in packed with either molecular sieve 13X or 5A, depending on the quantity of air present. C_2H_6 was separated on a stainless steel column of the same dimensions packed with Porapak QS. All columns were operated at room temperature with a helium flow rate of 35 cm^3 min^{-1}.

Propionaldehyde, obtained from Aldrich, was purified by trap-to-trap distillation from −63 to −161 °C. The air, oxygen, nitrogen, CO and C_2H_6 used were Matheson zero gas, extra dry, prepurified, chemically pure and chemically pure grades respectively.

Experiments were performed at 254, 280, 302, 313, 326 and 334 nm. For experiments performed at 326 nm, a cadmium vapor resonance lamp powered by a Philips spectral lamp supply was used in conjunction with a Corning 0-54 cut-off filter. This filter removed the cadmium 228 nm resonance line allowing only the 326 nm line to pass. For experiments performed at 254 nm a Hanovia low pressure mercury lamp was used. The 185 nm resonance line was removed by absorption in air before striking the cell. In all other experiments a Hanovia medium pressure mercury lamp and lamp stabilizer were used. The 313 and 334 nm mercury lines were isolated with Corion SM-3130-2 and SM-3340-2 interference filters respectively. The bandwidth (full width at half-maximum) of these filters is approximately 8 nm. In experiments performed at 280 and 302 nm the mercury lamp output was focused on the entrance slit of a Jarrell Ash 0.25 m Ebert monochromator. Both entrance and exit slits were 2 mm wide. The bandpass of the monochromator was 7.5 nm under these conditions. From the measured lamp intensities at 297 and 302 nm it was determined that, with the monochromator set at 302 nm, 14% of the light passing through the exit slit was from the 297 nm line. For experiments at 280 nm, 3% and 7.6% of the light passed by the monochromator was at 289 nm and 275 nm respectively.

In experiments performed at 326 and 334 nm, azomethane was used as an actinometer. The N_2 produced from the photolysis of azomethane was measured by gas chromatography on molecular sieve 13X. The azomethane was prepared using a modified procedure reported by Renaud and Leitch [11]. It was purified by trap-to-trap distillation from −89 to −161 °C. For the experiments performed at 254 nm phosgene was used as the actinometer. The CO produced from the photolysis of phosgene was separated on the molecular sieve 13X column. Air Products chemically pure grade phosgene was used after distillation from −90 to −127 °C. The pressure of azomethane or phosgene used in the actinometry experiments was determined by matching absorbances with the pressure of propionaldehyde used in each experiment. Actinometry was performed before and after each experiment.

Since the quantum yield for CO production at 254, 334, 326 and 313 nm [7] in the low pressure limit was found to be unity, "actinometry" at 280 and 302 nm was performed by photolyzing about 3 Torr of propionaldehyde in the presence of about 2 Torr of oxygen and assuming that the CO quantum yield was unity under these conditions.

Mass spectra of all purified reagents were obtained and compared with the EPA–NIH mass spectral data base. In all cases no extraneous peaks were present.

3. Results

In the presence of oxygen, or in this case air, both primary processes lead to the production of CO and process (2) also leads to C_2H_6. At low conversion these are the only sources of CO and C_2H_6 [7]. Thus $\Phi(C_2H_6)$ is a measure of primary process (2), and $\Phi(CO) - \Phi(C_2H_6)$ is a measure of primary process (1).

The CO and C_2H_6 quantum yields at each wavelength studied are reported in Table 1. The pressure of propionaldehyde in each experiment is 10.1 ± 0.1 Torr. The CO quantum yield $\Phi(CO)$ decreases with increasing pressure of air from a value of approximately 1.0 at low pressures. Significant amounts of C_2H_6 were produced only at 254 and 280 nm. At 254 nm the C_2H_6 quantum yield $\Phi(C_2H_6)$ is independent of pressure, and $\Phi(C_2H_6) = 0.39 \pm 0.02$. At 280 nm, $\Phi(C_2H_6) = 0.33$ in the limit of zero pressure and decreases with increasing pressure of air to a limiting value of about 0.050 above atmospheric pressure. The quenchable fraction, *i.e.* $\Phi(C_2H_6) - 0.050$, exhibits Stern–Volmer kinetics, as shown in Fig. 1.

The free-radical process $\Phi(rad) = \Phi(CO) - \Phi(C_2H_6)$ decreases as the pressure increases. This is shown graphically at each wavelength in Figs. 2 - 7 where $\Phi(rad)^{-1}$ is plotted against the equivalent total air pressure $[M] \equiv [N_2] + [O_2] + 1.5[C_2H_5CHO]$ [7]. Except at the two lower wavelengths, C_2H_6 is not produced, so that $\Phi(rad)$ is taken as $\Phi(CO)$. The Stern–Volmer plots of $\Phi(rad)^{-1}$ *versus* [M] are linear at four wavelengths but show marked

TABLE 1

Effect of air pressure on the photolysis of C_2H_5CHO[a]

Air pressure (Torr)	*Irradiation time* (h)	$I_a \times 10^{-11}$ (photons $cm^{-3} s^{-1}$)	$\Phi(CO)$	$\Phi(C_2H_6)$
λ = *334 nm*				
7.04	1.0	1.08	0.75	—
16.3	2.0	0.84	0.63	—
25.6	3.0	0.87	0.53	—
44.7	4.5	1.02	0.51	—
90.0	7.5	0.90	0.46	—
140	11.58	0.87	0.41	—
190	16.0	0.93	0.38	—
340	19.0	0.87	0.29	$<9 \times 10^{-3}$
λ = *326 nm*				
5.50	1.5	0.430	0.77	—
27.0	3.3	0.398	0.56	—
44.1	5.0	0.411	0.52	—
65.0	10.3	0.405	0.45	—
100	12.0	0.407	0.31	—
175	22.1	0.424	0.23	—
290	36.0	0.433	0.159	<0.015
λ = *313 nm*				
7.30	0.25	8.14	0.83	—
38.1	0.50	8.25	0.66	—
85.0	1.00	6.11	0.66	—
135	1.16	6.24	0.52	—
280	1.50	6.62	0.42	—
425	2.08	5.79	0.33	—
570	2.00	6.97	0.30	—
713	2.50	7.67	0.26	—
λ = *302 nm*				
7.31	1.0	1.87	0.79	0.029
36.3	1.5	1.74	0.66	0.027
65.2	2.8	1.59	0.57	—
130	3.0	1.62	0.60	—
239	3.5	1.63	0.45	—
419	5.0	1.78	0.33	—
704	6.0	1.68	0.23	—
λ = *280 nm*				
7.30	2.5	0.716	0.79	0.233
38.6	4.0	0.714	—	0.172
85.0	9.0	0.439	0.73	0.167
135	8.0	0.539	0.56	0.128
279	13.0	0.426	0.48	0.093
427	12.0	0.672	0.51	0.084
570	10.0	0.701	0.41	0.076
712	15.3	0.602	0.37	0.070

(continued)

TABLE 1 *(continued)*

Air pressure (Torr)	*Irradiation time* (h)	$I_a \times 10^{-11}$ (photons cm^{-3} s^{-1})	$\Phi(CO)$	$\Phi(C_2H_6)$
λ = *254 nm*				
6.77	0.33	6.22	0.93	0.438
21.8	0.42	6.01	0.83	0.386
35.5	0.50	6.01	0.75	0.408
80.2	0.92	6.01	0.71	0.377
190	1.75	6.01	0.64	0.380
390	2.00	5.95	0.57	0.380
627	2.33	6.12	0.53	0.390

[a] The pressure of C_2H_5CHO is 10.1 ± 0.1 Torr.

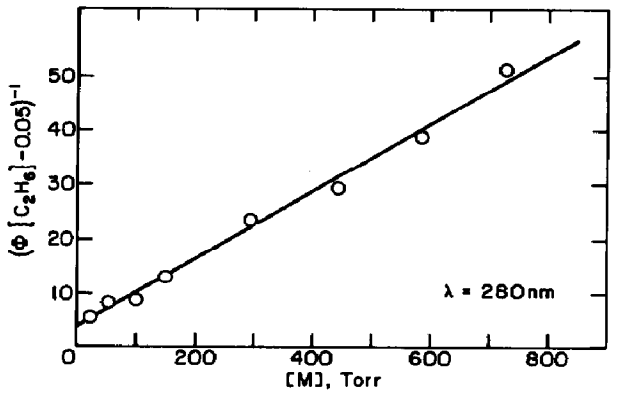

Fig. 1. Plot of $\{\Phi(C_2H_6) - 0.05\}^{-1}$ *vs.* total pressure at 280 nm.

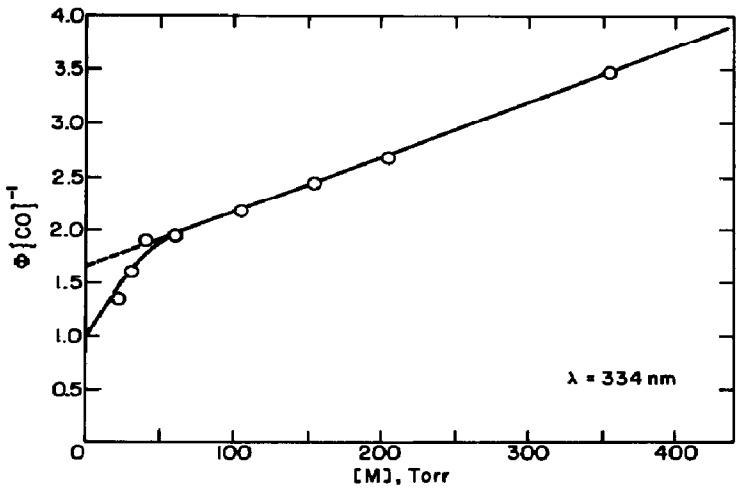

Fig. 2. Plot of the reciprocal CO quantum yield *vs.* total pressure at 334 nm.

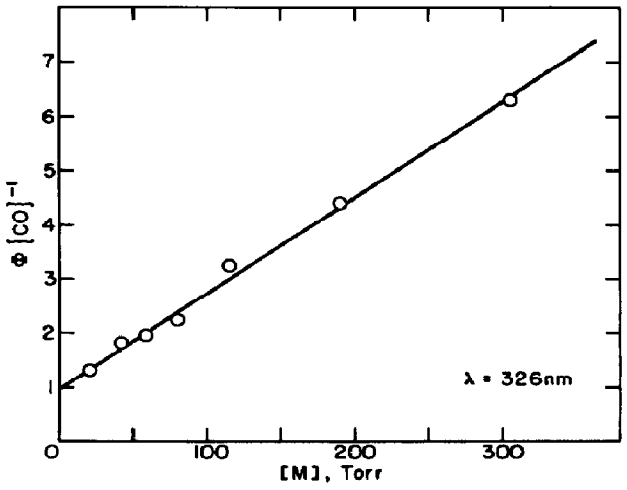

Fig. 3. Plot of the reciprocal CO quantum yield *vs.* total pressure at 326 nm.

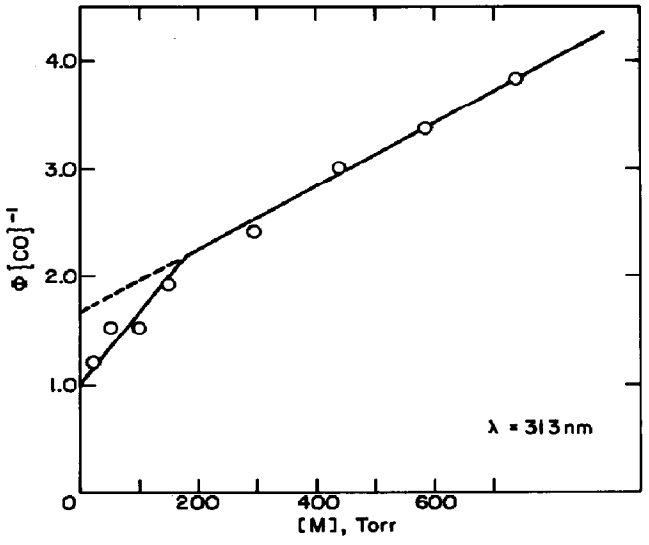

Fig. 4. Plot of the reciprocal CO quantum yield *vs.* total pressure at 313 nm.

curvature at 334 and 313 nm. The same deviation from linearity at 313 nm was seen in another study performed with a different apparatus [7]. Thus there is a remarkable wavelength dependence on the quantum yield quenching characteristics.

4. Discussion

Both primary photochemical processes show complex behavior. All the evidence suggests that the radical-producing process takes place through the triplet state in agreement with phosphorescence data on acetaldehyde [12]

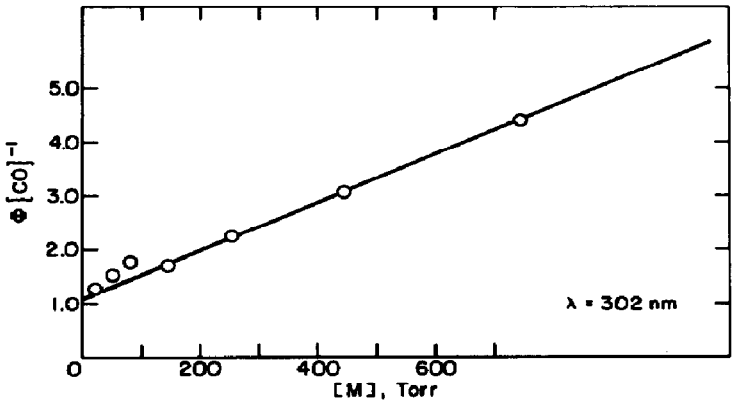

Fig. 5. Plot of the reciprocal CO quantum yield *vs.* total pressure at 302 nm.

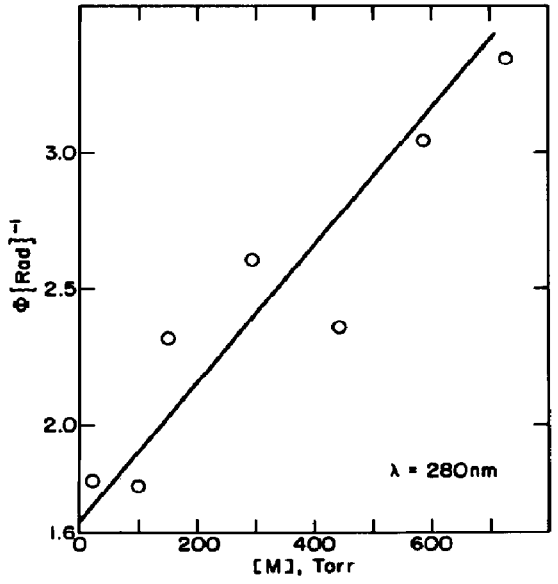

Fig. 6. Plot of the reciprocal quantum yield for the radical-producing step at 280 nm.

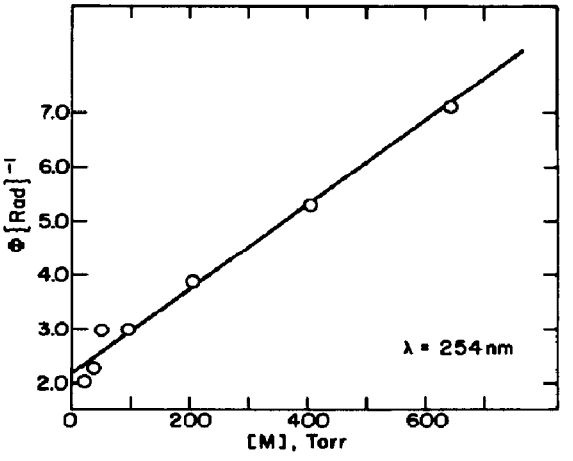

Fig. 7. Plot of the reciprocal quantum yield for the radical-producing step at 254 nm.

and propionaldehyde [13] and with intersystem crossing yields determined for butyraldehyde [14]. The work of Parmenter and Noyes [12] indicates that the acetaldehyde triplet state formation yield is unity at longer wavelengths. From their observations of HCO formation times, Gill and Atkinson [4] ruled out the acetaldehyde ^1A state as the precursor to process (1). Although it is believed that some dissociation comes from upper vibrational levels of the singlet state at shorter wavelengths [3, 4] and that both the singlet and triplet states exist [6], it is unclear what fraction of each contributes to photolysis at each wavelength.

Borkowski and Ausloos [13] found the room temperature fluorescence yields of C_2H_5CHO to be almost unaffected by changes in pressure. However, the yields did show a slight increase with pressure at 280.4 nm and a

slight decrease with increasing pressure at 334 nm, with essentially no pressure effect at 313 nm. Whether or not the trends at 280.4 and 334 nm are meaningful, they are small (a 68% increase at 280.4 nm for an increase by a factor of 13.9 in pressure and a 27% decrease at 334 nm for an increase in pressure by a factor of 10). To simplify our analysis we shall assume that these changes are negligible and that the fluorescence yield is not affected by pressure changes. However, the triplet yield, as measured by the sensitization of biacetyl phosphorescence, increased by a factor of 3 - 4 as the C_2H_5CHO pressure was increased from 25 to 100 Torr at 313 nm, but there was only a 10% - 20% increase of the triplet yield at 334 nm for C_2H_5CHO pressure increases of between 21 and 108 Torr. Thus the decrease in radical yield with increasing pressure can be considered to lead to an increase in triplet states which can sensitize biacetyl phosphorescence, *i.e.* low vibrational levels of the triplet state.

The production of C_2H_6 via process (2) is important only at 254 and 280 nm. From the data at 280 nm it is clear that there are both quenchable and non-quenchable contributions to C_2H_6 production. At 280 nm the quantum yield for the non-quenchable fraction is 0.050 ± 0.001. It is generally believed that the molecular process occurs through upper vibrational levels of either the first excited singlet state or the ground state or both. We propose that the quenchable fraction occurs through excited vibrational levels of the ground state singlet and that the non-quenchable fraction occurs through the first excited singlet.

It is also clear that the radical process proceeds from two states, at least at 313 and 334 nm, both of which are pressure quenched. Also pressure quenching increases the C_2H_5CHO triplet yield. Thus at least one of the radical-producing states can be associated with high vibrational levels of the triplet state. In our earlier work [7] we considered both radical precursor states to be upper vibrational levels of the triplet with different quenching efficiencies.

A general mechanism accounting for all the above-mentioned processes is given below. The rate coefficients for each first-order process may be a function of wavelength:

$$P + h\nu \rightarrow {}^1P \qquad \text{rate, } I_a$$

$$^1P \rightarrow C_2H_6 + CO \tag{4}$$

$$^1P \rightarrow P_0^* \tag{5}$$

$$P_0^* \rightarrow C_2H_6 + CO \tag{6}$$

$$P_0^* + M \rightarrow \text{deactivation} \tag{7}$$

$$^1P \rightarrow {}^3P_I \tag{8}$$

$$^1P \rightarrow {}^3P_{II} \tag{9}$$

$$^3P_I \rightarrow C_2H_5 + HCO \tag{10}$$

$$^3P_I + M \rightarrow \text{deactivation} \tag{11}$$

$$^3P_{II} \rightarrow C_2H_5 + HCO \quad (12)$$

$$^3P_{II} + M \rightarrow \text{deactivation} \quad (13)$$

where ^1P, P_0^*, ^3P_I and $^3P_{II}$ represent respectively the excited singlet state, the vibrationally excited ground state, and the more reactive and the less reactive levels of the vibrationally excited triplet state. This mechanism leads to the following rate law for the primary processes which produce free radicals:

$$\Phi(\text{rad}) = \frac{\phi_8}{1 + k_{11}[M]/k_{10}} + \frac{\phi_9}{1 + k_{13}[M]/k_{12}} \quad (14)$$

The rate law for the molecular process is given by

$$\Phi(C_2H_6) = \phi_4 + \frac{\phi_5}{1 + k_7[M]/k_6} \quad (15)$$

With the realization that ϕ_4, ϕ_5, ϕ_8 and ϕ_9 are independent of pressure, the rate coefficient ratios k_{11}/k_{10}, k_{13}/k_{12} and k_7/k_6 can be computed for each wavelength as shown below. For the four longer wavelengths the molecular process is unimportant and $\Phi(\text{rad}) = \Phi(CO)$.

4.1. 334 and 313 nm

At very high pressures the slowly reacting levels of the vibrationally excited triplet state $^3P_{II}$ are unimportant, *i.e.* k_{12} is very much less than $k_{13}[M]$, and eqn. (14) reduces to

$$\Phi(CO)^{-1} \approx \phi_8^{-1}\left(1 + \frac{k_{11}[M]}{k_{10}}\right) \quad (16)$$

From the high pressure portion of the plots in Figs. 2 and 4, the ratio of slope to intercept gives k_{10}/k_{11} values of 325 Torr and 570 Torr respectively at 334 nm and 313 nm, and the intercepts give $\phi_8 = 0.60$ at both wavelengths. The values at 313 nm are in excellent agreement with our previous work [7] in which we found $\phi_8 = 0.60$ and $k_{10}/k_{11} = 625$ Torr.

Equation (14) can be rearranged to give

$$\left\{\Phi(CO) - \frac{\phi_8}{1 + k_{11}[M]/k_{10}}\right\}^{-1} = \phi_9^{-1}\left(1 + \frac{k_{13}[M]}{k_{12}}\right) \quad (17)$$

In principle the left-hand side of eqn. (17) can be plotted against [M] to obtain k_{13}/k_{12} since $\phi_9 = 1 - \phi_8 = 0.40$. In practice, only the few data points in the lower left-hand corners of Figs. 2 and 4 are useful in plotting eqn. (17) and these have considerable scatter. However, if smooth curves are drawn through these points passing through unity as an intercept, then "optimized" values of $\Phi(CO)$ can be estimated for use in computing the left-hand side of eqn. (17). Plots were made in this manner (not shown) and from them k_{12}/k_{13} was estimated to be about 24 Torr at 334 nm and about 45 Torr at 313 nm. The latter value can be compared with the value of 70 Torr found from more extensive data in our earlier work [7].

Estimates of k_{12}/k_{13} can also be made from the pressure enhancement of biacetyl phosphorescence in the C_2H_5CHO-sensitized emission of biacetyl

[13]. From the data of Borkowski and Ausloos k_{12}/k_{13} can be estimated to be about 50 Torr at 313 nm and less than 20 Torr at 334 nm with C_2H_5CHO as the quenching gas. Since C_2H_5CHO is about 1.5 times as efficient as oxygen or nitrogen as a quenching gas [7], the corresponding values corrected to air would be comparable with our values.

4.2. 326 and 302 nm

At these wavelengths the Stern–Volmer plots in Figs. 3 and 5 show no deviation from linearity. Thus either ϕ_8 or ϕ_9 is zero, and the slope of the Stern–Volmer plot gives either k_{11}/k_{10} or k_{13}/k_{12}. The values obtained for the reciprocal slope are 57 Torr and 225 Torr respectively at 326 nm and 302 nm. These values correspond to low reactivity so that we assume that $\phi_8 = 0$ and $\phi_9 = 1.0$.

4.3. 280 and 254 nm

At 280 and 254 nm the molecular process becomes important, and Φ(rad) must be computed as $\Phi(CO) - \Phi(C_2H_6)$. This function gives linear Stern–Volmer plots (Figs. 6 and 7) although the data at 280 nm are badly scattered. Thus either ϕ_8 or ϕ_9 is zero. The ratio of slope to intercept gives relative half-quenching pressures (k_{10}/k_{11} or k_{12}/k_{13}) of 610 Torr and 280 Torr at 280 nm and 254 nm respectively. Since the half-quenching pressure should increase monotonically with the input energy, we assign the value of 610 Torr at 280 nm to the slow quench k_{10}/k_{11} and the value of 280 Torr at 254 nm to the rapid quench k_{12}/k_{13}. The intercepts of Figs. 6 and 7 give respectively $\phi_8 = 0.61$ at 280 nm ($\phi_9 \approx 0$) and $\phi_9 = 0.46$ at 254 nm ($\phi_8 \approx 0$).

The rate law for the molecular process is given by eqn. (15). At 254 nm there is no pressure dependence, $\phi_5 \approx 0$ and $\phi_4 \approx \Phi(C_2H_6) = 0.39 \pm 0.03$. The sum of the quantum yields $\phi_4 + \phi_9 = 0.85$ at 254 nm, whereas we expect a value of 1.0. The discrepancy between 0.85 and 1.0 may just reflect the uncertainty in our measurements. Alternatively it may represent another very rapidly quenched free-radical-producing step present at 254 nm.

At 280 nm both ϕ_4 and ϕ_5 are non-zero. Equation (15) can be rearranged to

$$\{\Phi(C_2H_6) - \phi_4\}^{-1} = \phi_5^{-1}\left(1 + \frac{k_7[M]}{k_6}\right) \tag{18}$$

If ϕ_4 is taken to be 0.050, a linear Stern–Volmer plot results as shown in Fig. 1. From the slope and intercept we obtain $k_6/k_7 = 47$ Torr and $\phi_5 = 0.28$. At this wavelength the sum of the quantum yields $\phi_4 + \phi_5 + \phi_8$ is about 1.0, thus accounting for all the primary processes.

A summary of the rate coefficients and quantum yields is given in Table 2. At all wavelengths the sum of the quantum yields $\phi_4 + \phi_5 + \phi_8 + \phi_9$ is about 1.0, except possibly at 254 nm. The more reactive triplet states appear only at 334, 313 and 280 nm, and always with a quantum yield ϕ_8 of 0.60. These states do not seem to appear at 326, 302 or 254 nm. The less

TABLE 2

Summary of the rate coefficient ratios and quantum yields

λ (nm)	k_{10}/k_{11} (Torr)	k_{12}/k_{13} (Torr)	k_6/k_7 (Torr)	ϕ_4	ϕ_5	ϕ_8	ϕ_9
334	325	≈ 24	—	—	—	0.60	0.40
326	—	57	—	—	—	—	1.0
313	570[a]	≈ 45[a]	—	—	—	0.60	0.40
302	—	225	—	0.028	—	—	1.0
280	610	—	47	0.050	0.28	0.61	—
254	—	280	—	0.39	—	—	0.46

[a] We found k_{10}/k_{11} = 630 Torr and k_{12}/k_{13} ≈ 70 Torr in earlier work at 313 nm [7].

reactive triplet states appear at 334 and 313 nm with a quantum yield of 0.4, about the same value as found for the sum of the quantum yields for the molecular processes at the lowest two wavelengths.

5. Atmospheric implication

One goal of this work was to calculate the photodissociation rate coefficient for radical production under atmospheric conditions. This rate coefficient k_{rad} is given by

$$k_{rad} = \int I_0 \epsilon \Phi(\text{rad})\, d\lambda \qquad (6)$$

where I_0 is the incident photon flux at each wavelength λ and ε is the extinction coefficient (to base e) at each wavelength. Values for Φ(rad) at atmospheric pressure at each wavelength examined in this study are listed in Table 3. There is no smooth trend to the data, so it is difficult to estimate Φ(rad) at other wavelengths. However, to a first approximation Φ(rad) can be considered to be about 0.20 ± 0.08 at all wavelengths.

TABLE 3

Quantum yield for primary process (1) in air at 760 Torr

λ (nm)	Φ(rad)
334	0.18
326	0.067
313	0.26
302	0.22
280	0.28
254	0.13

Values of ϵ and I_0 at two zenith angles χ over wavelength intervals are given in Table 4. With these data and the assumption that $\Phi(\text{rad}) \approx 0.20$ at all wavelengths, k_{rad} is computed to be 1.3×10^{-5} s^{-1} at $\chi = 30°$ and 9.7×10^{-6} s^{-1} at $\chi = 58.18°$.

TABLE 4

Data for evaluating atmospheric photodissociation rate coefficients for propionaldehyde

λ (nm)	ϵ[a] (cm^2 molecule^{-1})	I_0[b] (photons cm^{-2} s^{-1})	
		$\chi = 30°$	$\chi = 58.18°$
335.0 - 340.0	1.38×10^{-21}	1.119×10^{15}	1.081×10^{15}
330.0 - 335.0	4.83×10^{-21}	1.039×10^{15}	9.883×10^{14}
325.0 - 330.0	8.80×10^{-21}	1.075×10^{15}	9.928×10^{14}
320.0 - 325.0	1.27×10^{-20}	8.309×10^{14}	7.289×10^{14}
315.0 - 320.0	2.03×10^{-20}	6.104×10^{14}	4.847×10^{14}
310.0 - 315.0	3.44×10^{-20}	4.154×10^{14}	2.803×10^{14}
307.7 - 310.0	3.69×10^{-20}	2.327×10^{14}	1.088×10^{14}
303.0 - 307.7	4.07×10^{-20}	7.330×10^{13}	1.771×10^{13}
298.5 - 303.0	5.11×10^{-20}	9.368×10^{12}	7.001×10^{11}
294.1 - 298.5	5.34×10^{-20}	4.315×10^{11}	4.273×10^{9}
289.9 - 294.1	5.93×10^{-20}	2.566×10^{9}	8.83×10^{5}

[a] From McMillan as reported by Calvert and Pitts [2].
[b] From Wuebbles [15].

Acknowledgment

This work was supported by the Atmospheric Sciences Section of the National Science Foundation through Grant ATM-7909169 for which we are grateful.

References

1 A. C. Lloyd, *NBS Spec. Publ. 557*, 1979, p. 27 (National Bureau of Standards, U.S. Department of Commerce).
2 J. G. Calvert and J. N. Pitts, Jr., *Photochemistry*, Wiley, New York, 1966.
3 E. K. C. Lee and R. S. Lewis, *Adv. Photochem., 12* (1980) 1.
4 R. J. Gill and G. H. Atkinson, *Chem. Phys. Lett., 64* (1979) 426.
5 F. E. Blacet and J. N. Pitts, Jr., *J. Am. Chem. Soc., 74* (1952) 3382.
6 D. A. Hansen and E. K. C. Lee, *J. Chem. Phys., 63* (1975) 3272.
7 P. B. Shepson and J. Heicklen, *J. Photochem., 18* (1982) 169.
8 J. Weaver, J. Meagher and J. Heicklen, *J. Photochem., 6* (1976) 111.
9 F. Su, J. G. Calvert and J. H. Shaw, *J. Phys. Chem., 83* (1979) 3185.
10 J. P. Reilly, J. H. Clark, C. B. Moore and G. C. Pimentel, *J. Chem. Phys., 69* (1978) 4381.
11 R. Renaud and L. C. Leitch, *Can. J. Chem., 32* (1954) 549.
12 C. S. Parmenter and W. A. Noyes, Jr., *J. Am. Chem. Soc., 85* (1963) 416.
13 R. P. Borkowski and P. Ausloos, *J. Am. Chem. Soc., 84* (1962) 4044.
14 S. Förgeteg, S. Dóbé and T. Bérces, *React. Kinet. Catal. Lett., 9* (1978) 331.
15 D. Wuebbles, personal communication, 1981.